Environmental Science & Technology

Article

pubs.acs.org/est

Bioreduction of Hydrogen Uranyl Phosphate: Mechanisms and U(IV) Products

Xue Rui,[†,⊥] Man Jae Kwon,[‡,§,⊥] Edward J. O'Loughlin,[‡] Sarrah Dunham-Cheatham,[∥] Jeremy B. Fein,[∥] Bruce Bunker,[†] Kenneth M. Kemner,[‡] and Maxim I. Boyanov*[,‡]

[†]Department of Physics, University of Notre Dame, Notre Dame, Indiana 46556, United States

[‡]Biosciences Division, Argonne National Laboratory, Argonne, Illinois 60439, United States

[§]Korea Institute of Science and Technology, Gangneung 210-340, S. Korea

[∥]Department of Civil and Environmental Engineering and Earth Sciences, University of Notre Dame, Indiana 46556, United States

Supporting Information

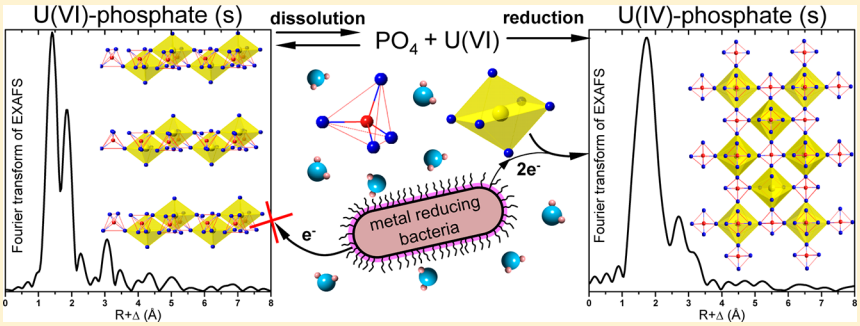

ABSTRACT: The mobility of uranium (U) in subsurface environments is controlled by interrelated adsorption, redox, and precipitation reactions. Previous work demonstrated the formation of nanometer-sized hydrogen uranyl phosphate (abbreviated as HUP) crystals on the cell walls of *Bacillus subtilis*, a non-U^{VI}-reducing, Gram-positive bacterium. The current study examined the reduction of this biogenic, cell-associated HUP mineral by three dissimilatory metal-reducing bacteria, *Anaeromyxobacter dehalogenans* strain K, *Geobacter sulfurreducens* strain PCA, and *Shewanella putrefaciens* strain CN-32, and compared it to the bioreduction of abiotically formed and freely suspended HUP of larger particle size. Uranium speciation in the solid phase was followed over a 10- to 20-day reaction period by X-ray absorption fine structure spectroscopy (XANES and EXAFS) and showed varying extents of U^{VI} reduction to U^{IV}. The reduction extent of the same mass of HUP to U^{IV} was consistently greater with the biogenic than with the abiotic material under the same experimental conditions. A greater extent of HUP reduction was observed in the presence of bicarbonate in solution, whereas a decreased extent of HUP reduction was observed with the addition of dissolved phosphate. These results indicate that the extent of U^{VI} reduction is controlled by dissolution of the HUP phase, suggesting that the metal-reducing bacteria transfer electrons to the dissolved or bacterially adsorbed U^{VI} species formed after HUP dissolution, rather than to solid-phase U^{VI} in the HUP mineral. Interestingly, the bioreduced U^{IV} atoms were not immediately coordinated to other U^{IV} atoms (as in uraninite, UO_2) but were similar in structure to the phosphate-complexed U^{IV} species found in ningyoite [$CaU(PO_4)_2 \cdot H_2O$]. This indicates a strong control by phosphate on the speciation of bioreduced U^{IV}, expressed as inhibition of the typical formation of uraninite under phosphate-free conditions.

INTRODUCTION

The mobility of U in subsurface environments is controlled by a number of adsorption, precipitation, and redox reactions, often resulting from microbial activity. Oxidized U^{VI} species, such as the hydrated uranyl cation (UO_2^{2+}) or the uranyl-carbonate complexes ($UO_2(CO_3)_n^{(2-2n)}$), are relatively soluble in aquatic systems, and this can lead to the development of highly dispersed contaminant plumes.[1−5] Efforts to mitigate the migration of U in subsurface environments have largely focused on approaches that decrease U solubility (and thus mobility), including reduction of U^{VI} to U^{IV} with subsequent precipitation of sparingly soluble U^{IV} phases, as well as addition of amendments that induce precipitation of sparingly soluble U^{VI} minerals. Reductive approaches for U immobilization rely on the formation of low-solubility U^{IV} phases such as uraninite (UO_2). Both laboratory and field-scale experiments have demonstrated the ability of a phylogenetically diverse range of microorganisms (primarily Fe^{III}- or sulfate-reducing bacteria) to reduce U^{VI} to uraninite, thereby lowering dissolved U concentrations.[6−15] However, the long-term stability of the U^{IV} phases is uncertain, especially if conditions become oxic and

Received: December 21, 2012
Revised: May 1, 2013
Accepted: May 1, 2013
Published: May 1, 2013

 © 2013 American Chemical Society

U^{IV} phases such as uraninite become susceptible to oxidation back to soluble/mobile U^{VI}.[16−25]

An alternative approach involving the addition of dissolved phosphate or phosphate-bearing minerals (e.g., apatite) to induce the formation of low-solubility uranyl phosphate minerals has also been explored. Indeed, the potential for U^{VI} immobilization by phosphate amendments has been demonstrated in both laboratory and field-scale experiments,[26−39] which typically report the precipitation of uranyl phosphate phases belonging to the autunite and meta-autunite groups, such as $(Na,Ca)_{2-1}[(UO_2)(PO_4)_2]\cdot 3H_2O$ or chernikovite $[(H_3O)_2(UO_2)_2(PO_4)_2\cdot 6H_2O]$. Autunite and meta-autunite minerals are common in a wide variety of U deposits[40] and have been identified in soils and subsurface sediments from U-contaminated sites.[41,42]

Studies of naturally formed autunite/meta-autunites suggest that they are a stable sink for U.[43,44] However, as with reductive precipitation approaches, uncertainty remains regarding the fate of U precipitated as U^{VI}-phosphate. Aerobic bacteria are known to promote the dissolution of phosphate-bearing minerals, including autunite, as a means of obtaining phosphate.[45−48] Besides dissolution, uranyl phosphates may also become subject to reducing conditions. For instance, the uranium ore deposit at Coles Hill, VA, exhibits a sharp redox front containing U^{VI}-phosphate and reduced U^{IV} species on each side.[43] At such redox boundaries colloidal U^{VI}-phosphates may be transported to the reducing zone together with groundwater movement. In remediation approaches aimed at uranyl phosphate precipitation by bacteria capable of phosphatase activity,[27−29,31,32,35] it is possible that stimulation of the subsurface microbial community with glycerol-3-phosphate will result in concurrent stimulation of metal-reducing strains. Even isolated strains of bacteria exhibiting phosphatase activity have been shown to produce both U^{VI}-phosphate and reduced U^{IV}.[49,50] The dynamics between U^{VI}-phosphate precipitation and reduction may also affect the reduction kinetics or U speciation in approaches focused solely on U^{VI} bioreduction—phosphate may already be present at a field site, or it may be supplied in the treatment to ameliorate phosphate limitations during the biostimulation activities. All of the above have the potential to produce U^{VI}-phosphate before or during the establishment of reducing conditions.

Overall, the fate of uranyl phosphates under reducing conditions and the effect of U^{VI}-phosphate precipitation on the bioreduction of U^{VI} are unclear. Smeaton et al.[51] reported no reduction of U^{VI} in meta-autunite by *Shewanella putrefaciens* strain 200R, a Gram-negative, dissimilatory U^{VI}-reducing bacterium.[52] Similarly, the release of phosphate following hydrolysis of intracellular polyphosphate and subsequent precipitation of uranyl phosphate appeared to limit the reduction of U^{VI} by the Gram-positive, metal-reducing bacteria *Pelosinus* sp. UFO1 and *Cellulomonas* sp. ES6.[49,50] In contrast, the thermophilic, Gram-positive bacterium *Carboxydothermus ferrireducens* (previously classified as *Thermoterrabacterium ferrireducens*) readily reduced U^{VI} present as the meta-autunite mineral uramphite to U^{IV}, with the subsequent precipitation of the U^{IV} phosphate mineral ningyoite $[CaU(PO_4)_2\cdot H_2O]$.[53] These conflicting results make it difficult to characterize definitively the transformations of U^{VI} phosphate minerals in natural systems under reducing conditions. In addition, biominerals formed in the presence of cell surfaces and exudates may have unexpected reactivity, as their properties are often different from those of their chemically precipitated counterparts.[54−56] It is also unclear whether bioreduction of solid U^{VI}-phosphates would produce the least-soluble form of U^{IV}, uraninite. Previous work suggests that dissolved phosphate inhibits uraninite formation during bioreduction of aqueous U^{VI},[7,49,50,57] resulting in the precipitation of ningyoite-like phases with relatively uncharacterized stability.[58] In this study we examine the potential for reduction of uranyl phosphate by *Anaeromyxobacter dehalogenans* strain K, *Geobacter sulfurreducens* strain PCA, and *Shewanella putrefaciens* strain CN32, all of which are Gram-negative, mesophilic, dissimilatory U^{VI}-reducing bacteria.[7,59−63] Two sources of solid-phase U^{VI} phosphate were examined: an abiotically precipitated, lower-surface-area uranyl hydrogen phosphate ($UO_2HPO_4\cdot 4H_2O$; abbreviated as HUP) and a biogenic, nanoparticulate HUP associated with the cell walls of *Bacillus subtilis* (a non-U^{VI}-reducing bacterium). The reduction of the two U^{VI} phosphate phases was compared under conditions either favoring or inhibiting HUP dissolution in order to evaluate the role of dissolved U^{VI} species, and the molecular structure of the reduced U^{IV} species was determined.

■ MATERIALS AND METHODS

Biogenic and Abiotic HUP Synthesis. The preparation and characterization of the *B. subtilis*-associated HUP and the abiotic HUP minerals were based on the methods used by Dunham-Cheatham et al.[55] modified as described in the Supporting Information. Precipitation of HUP in the presence of *B. subtilis* results in smaller (10−30 nm) particles agglomerated at the cell surface, whereas abiotic HUP precipitation results in freely suspended particles of larger size (50−150 nm). The mineral identity of the HUP phases was verified by X-ray diffraction and X-ray absorption spectroscopy, and the agglomeration of the biogenic HUP particles on the surface of *B. subtilis* was demonstrated in previous work.[55]

U^{VI} Bioreduction Experiments. Details on the culturing of *A. dehalogenans* K, *G. sulfurreducens* PCA, and *S. putrefaciens* CN-32 and on the setup of the bioreduction experiments are provided in the Supporting Information. Briefly, the anoxic experimental systems used for the U^{VI} reduction studies were prepared by sparging 60 mL of 30 mM bicarbonate buffered medium (±4.0 mM NaH_2PO_4) with N_2:CO_2 (= 80:20 for pH 6.8) or 60 mL of 30 mM HEPES buffered medium (±4.0 mM NaH_2PO_4) with Ar in 160-mL serum bottles. After sparging, the bottles were sealed with Teflon-lined rubber septa and aluminum crimp caps and sterilized by autoclaving. Acetate or lactate was provided as the sole electron donor for the metal-reducing bacteria (10−20 mM). One of the following U^{VI} forms was added as the sole electron acceptor: (1) *B. subtilis*-associated biogenic HUP (0.1 g wet mass with 5 mg of HUP mineral) or (2) abiotic HUP (5 mg of HUP mineral for each reactor). Total U^{VI} concentration was 0.2 mM for all reactors. The reactions were initiated by adding an aliquot of the desired metal-reducing cell suspension (0.07−0.1g of wet mass, 1.2−1.7 g L^{-1}).

HUP Dissolution. Experiments were performed to estimate the concentration of dissolved U in equilibrium with the biogenic and abiotic HUP phases under the solution conditions of our study. Identical reactors were prepared as described above for the bioreduction experiments, but the final step of inoculation with the metal-reducing bacteria was omitted. After 20 days of reaction, the concentration of U remaining in solution was determined by inductively coupled plasma-optical

Table 1. Extent of U^{VI} Reduction Obtained from Linear Combination Fitting of XANES and EXAFS Spectra

sample ID[a]	type of HUP	solution conditions	reaction period (days)	final U(aq) concn[b] (μM)	XANES U^{IV}/U_{total}[c] (%)	EXAFS U^{IV}/U_{total}[c] (%)
S. putrefaciens CN-32						
BSH	biogenic	HEPES	10	4.0	56	57
BSB	biogenic	bicarbonate	10	4.9	80	78
ASH	abiotic	HEPES	10	n.m.	21	27
ASB	abiotic	bicarbonate	10	n.m.	38	39
ASB-20	abiotic	bicarbonate	20	n.m.	67	59
BSH-PO_4	biogenic	HEPES + 4 mM PO_4	17	0.3	33	35
BSB-PO_4	biogenic	bicarbonate + 4 mM PO_4	17	<0.2	62	67
A. dehalogenans K						
BAH	biogenic	HEPES	10	9.4	22	24
BAB	biogenic	bicarbonate	10	8.6	53	52
AAH	abiotic	HEPES	10	n.m.	8	6
AAB	abiotic	bicarbonate	10	n.m.	43	41
AAB-20	abiotic	bicarbonate	20	n.m.	55	54
BAH-PO_4	biogenic	HEPES + 4 mM PO_4	17	0.3	11	12
BAB-PO_4	biogenic	bicarbonate + 4 mM PO_4	17	<0.21	21	26
G. sulfurreducens PCA						
BGH	biogenic	HEPES	10	4.3	29	29
BGB	biogenic	bicarbonate	10	3.1	100	-
AGH	abiotic	HEPES	10	n.m.	13	13
AGB	abiotic	bicarbonate	10	n.m.	42	40
AGB-20	abiotic	bicarbonate	20	n.m.	66	58
BGH-PO_4	biogenic	HEPES + 4 mM PO_4	17	<0.2	11	13
BGB-PO_4	biogenic	bicarbonate + 4 mM PO_4	17	<0.2	55	59

[a]The first letter represents the U source: B stands for biogenic HUP on the cell wall of *B. subtilis*, A for abiotically precipitated HUP. The second letter represents the metal reducer: S stands for *S. putrefaciens* CN-32, A for *A. dehalogenans* K, G for *G. sulfurreducens* PCA. The third letter represents the buffer solution: H stands for HEPES buffer, B for bicarbonate buffer. [b]Aqueous U concentrations measured by ICP-OES in the supernatants at the end of the reaction period. Measurement uncertainties are estimated to be <0.1 μM on the basis of the standard deviation from triplicate ICP measurements. n.m. = not measured. [c]Uncertainty in U^{IV}% from XANES fitting is estimated to be about 10%. Uncertainties from the EXAFS fitting were estimated to be 5% for all samples (see the Supporting Information). Although the XANES fitting procedure did not constrain the sum of the U^{VI} and U^{IV} proportions, the obtained sum was close to 1 (±0.05) for all samples.

emission spectroscopy (ICP-OES) with a PerkinElmer 4300DV instrument. The centrifugation supernatants (14,000g for 10 min) did not show any turbidity, indicating removal of the solids and colloids from solution.

Synchrotron Characterization. X-ray absorption near edge structure (XANES) spectra and extended X-ray absorption fine structure (EXAFS) spectra at the U L_{III}-edge (17,166 eV) were collected at the MRCAT/EnviroCAT bending magnet beamline[64] (sector 10-BM) at the Advanced Photon Source at Argonne National Laboratory. The hydrated pellets obtained by centrifugation of the suspensions were sealed inside Plexiglas slides with Kapton film windows and refrigerated until measurement, which occurred within 24 h. All samples were manipulated, stored, and measured under strict anoxic conditions. Spectra were recorded at room temperature in transmission and fluorescence modes by using gas-filled ionization detectors. To ensure data consistency and an absence of radiation-induced changes in U speciation, spectra were collected from three fresh locations, with three consecutive scans taken at each location. The spectrum for each sample was produced by averaging all consistent spectra. Further details on sample preparation, beamline setup, and data analysis can be found in the Supporting Information.

RESULTS AND DISCUSSION

U^{VI} Reduction Extent. The reduction extent was quantified by direct determination of U valence in the hydrated solid phases. All three metal-reducing bacteria reduced U^{VI} when incubated with biogenic or abiotic HUP; however, the extent of U^{VI} reduction depended on the bacterial species and the experimental conditions. The samples and conditions are described in Table 1. Selected U-L_{III} edge XANES spectra obtained with each bacterial species are compared to U^{VI} and U^{IV} standards in Figure 1. Spectra from the remaining samples in Table 1 are included in Figures S3 and S4, Supporting Information. Compared to the unreacted HUP spectrum, the reacted samples exhibit a shift in the absorption edge toward lower energy and dampening of the postedge shoulder feature. Both of the latter features indicate reduction of U^{VI} to U^{IV}.[65−67] Samples BGB and BSB (Table 1) showed the greatest extent of reduction, with XANES spectra similar to that of the U^{IV} standard.

The proportions of U^{IV} and U^{VI} components in the spectra were quantified by linear combination fitting. Table 1 and Figure S5 show the result of this analysis, demonstrating a good fit of the data. The transformation between the initial U^{VI} and final U^{IV} species is also evident in the $k^3\,\chi(k)$ EXAFS data shown in Figure 2. The EXAFS spectra exhibit consistent trends with the extents of reduction determined by XANES and show well-defined isosbestic points (points of identical molar absorption between samples, indicating that the spectra are resulting from changing proportions of the same two components). The isosbestic points are also present in comparisons of spectra for different metal-reducing bacteria (i.e., comparing spectra between panels 2A, 2B, and 2C). Linear combination analysis with U^{VI} and U^{IV} endmembers agrees well with the degree of U^{VI} reduction determined by XANES (Table

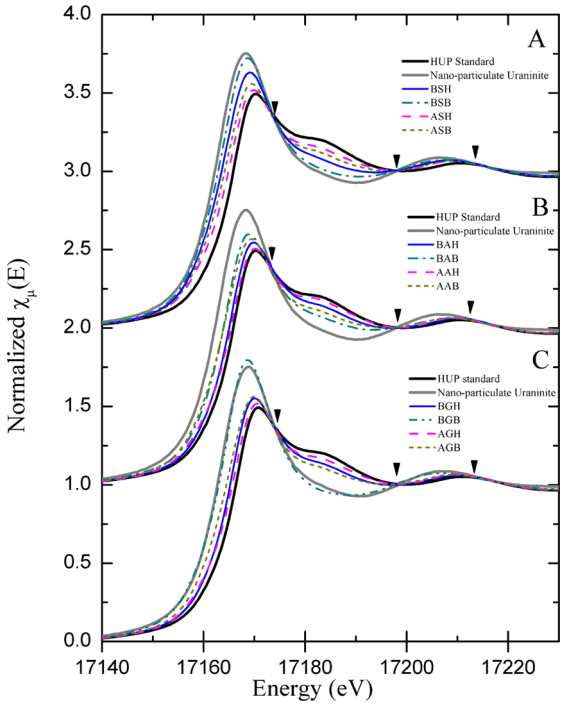

Figure 1. Uranium L_{III} edge XANES spectra from most of the bioreduction samples, compared to U^{VI} and U^{IV} endmember spectra (HUP and nanoparticulate uraninite, respectively). Spectra are offset vertically and grouped by metal-reducing bacteria: (A) *S. putrefaciens* CN-32, (B) *A. dehalogenans* K, (C) *G. sulfurreducens* PCA. Arrowheads indicate isosbestic points.

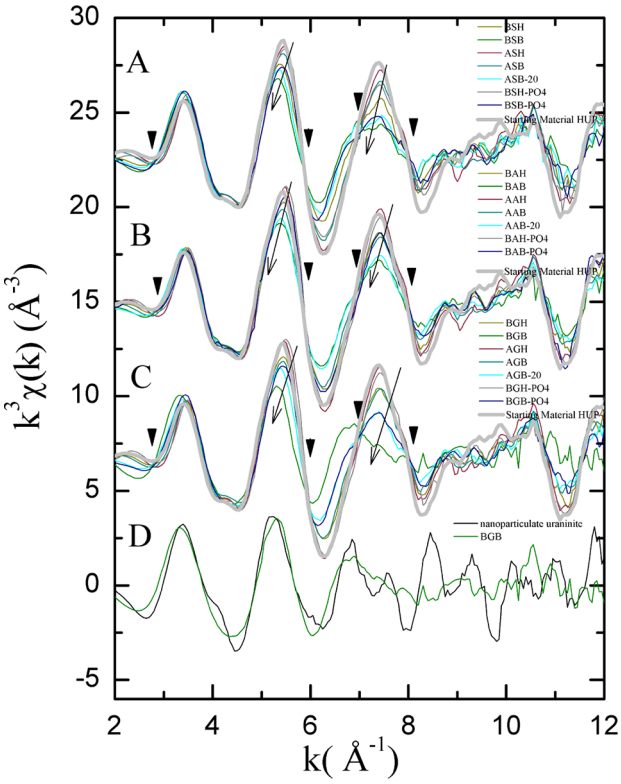

Figure 2. Uranium L_{III} edge k^3-weighted EXAFS spectra. Sample IDs are explained in Table 1. Spectra are offset vertically and grouped with respect to reducing bacteria species: (A) *S. putrefaciens* CN-32, (B) *A. dehalogenans* K, (C) *G. sulfurreducens* PCA. Arrows indicate the spectral trend with increasing extent of U transformation from HUP (thick gray line) to the reduced U^{IV} species. Isosbestic points are indicated by arrowheads. Spectra from the most reduced sample (BGB) and from nanoparticulate uraninite are compared in (D).

1 and Figure S6). All of the above suggest that U transformations occurred from the starting U^{VI} HUP species to a predominant, bacteria-independent U^{IV} endmember species, without the accumulation of a stable intermediate or other final U^{IV} species. Figure 2D compares the spectrum from the most reduced sample (BGB) to a spectrum from nanoparticulate uraninite, showing that the U^{IV} endmember species is not uraninite. The molecular structure of the U^{IV} species is analyzed in a separate section below.

Comparisons between the same samples reacted for different amounts of time show a greater extent of reduction with increased reaction time (e.g., ASB vs ASB-20, AAB vs AAB-20, AGB vs AGB-20 in Table 1 and Figure 3). The continuing evolution between 10 and 20 days of reaction time suggests slow kinetics of HUP reduction by the studied metal-reducing bacteria and ongoing U^{VI} reduction in all but one of the reactors. A detailed kinetic interpretation of the experiments was not possible with the limited number of synchrotron measurements available to probe the solid-to-solid redox transformations of U in our system. The interpretation of the data was therefore constrained to comparing the reduction extents over the same reaction period, assuming the same reaction mechanism in all systems. The analysis carried out under these limitations allows some trends to be observed in the effects of various parameters on the kinetics of HUP reduction.

Effect of Biogenic vs Abiotic HUP Source. Table 1 and Figure 3 demonstrate a consistent and significantly larger extent of U^{VI} reduction for biogenic HUP than for abiotic HUP, for the same amount of added U^{VI}. In the sample set without added phosphate, the reduction extent observed in *Shewanella* and *Geobacter* 10-day incubations was more than double with biogenic HUP than with abiotic HUP, in either HEPES or bicarbonate buffer. The same trend is observed with *Anaeromyxobacter* in HEPES buffer and, to a smaller extent, in bicarbonate buffer (U^{IV}/U_{total} = 53% vs 43% for biogenic vs abiotic HUP, Table 1). Incubations with *Anaeromyxobacter* and *Geobacter* in HEPES showed very limited reduction of the abiotic HUP mineral over 10 days (8% and 13%, respectively), whereas significant reduction was observed with the biogenic HUP mineral over the same period (22% and 29%, respectively). All of the above results indicate that biogenic HUP is reduced more extensively than abiotic HUP over similar reaction times, for all three bacterial species, in each of the examined buffers.

Effect of Bicarbonate. The data in Table 1 and Figure 3 demonstrate a larger extent of U^{VI} reduction in bicarbonate buffer than in HEPES. The reduction extent was 1.4 to 5.4 times greater in bicarbonate than in HEPES buffer for all three bacterial species, for both biogenic and abiotic HUP and for systems with or without added phosphate. Incubations with *Shewanella* showed the smallest increase in reduction extent with bicarbonate addition (1.4 to 1.9 times that for HEPES), whereas the effect of bicarbonate was more pronounced in the *Anaeromyxobacter* and *Geobacter* incubations (increase of 1.6 to 5.4 times). Comparisons of the reduction kinetics between different bacterial species was not possible because reactors were normalized to the same number of cells only within each metal-reducing species. The consistent results for all three

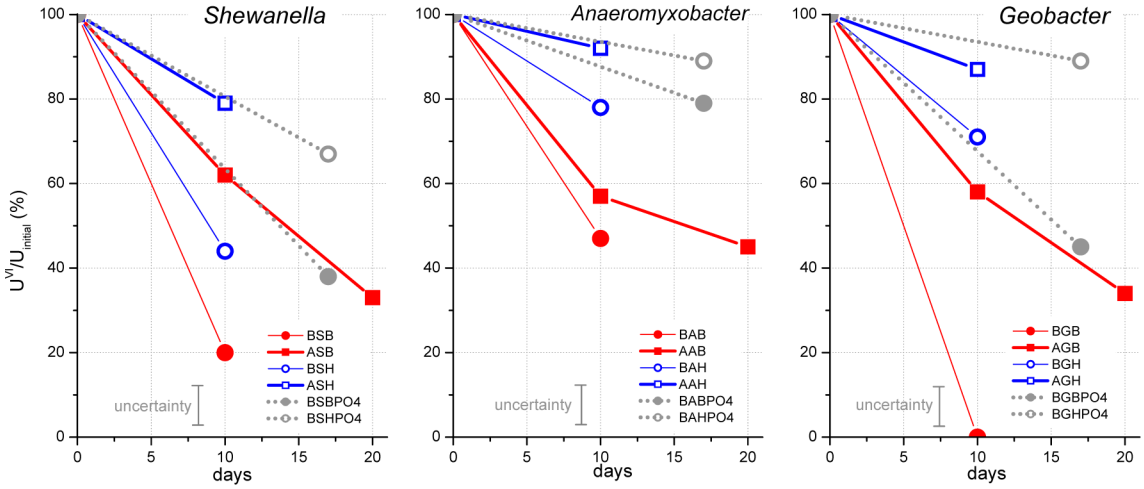

Figure 3. Percentage of U^{VI} in the solid phase over the studied reaction periods, as determined by fits of the XANES spectra. Sample descriptions and data are listed in Table 1. Data are labeled according to (1) the solution conditions (red, closed symbols = in bicarbonate solution; blue, open symbols = in HEPES solution; gray = bicarbonate or HEPES with additional 4 mM phosphate) and (2) the origin of the starting HUP mineral (circles, thin lines = biogenic HUP; squares, thick lines = abiotic HUP). The lines connecting the points provide a visual guide only. The uncertainty shown as a vertical bar is the same for all points and represents the uncertainty in valence determination from EXAFS.

metal-reducing species indicate that bicarbonate promoted more extensive U^{VI} reduction, for both biogenic and abiotic HUP. Bicarbonate enhancement of HUP bioreduction may also be expected at lower (1−2 mM) bicarbonate concentrations—typical field sites will also have lower U concentrations than the ones studied here, which would result in similarly high bicarbonate:U ratios and the predominance of the U^{VI}-carbonate aqueous complex.

Effect of Phosphate. The biogenic HUP reduction experiments were carried out with and without 4 mM dissolved phosphate added to the medium. The data in Table 1 and Figure 3 demonstrate that increasing the phosphate concentration above that resulting from HUP dissolution dramatically decreased the extent of U^{VI} reduction. All incubations with additional phosphate showed an extent of U^{VI} reduction that was 1.3 to 2.6 times less than that in corresponding systems without added phosphate, despite the longer reaction time allowed for the phosphate-amended systems. The extent of reduction of biogenic HUP by *Anaeromyxobacter* and *Geobacter* in the phosphate-amended HEPES-buffered medium was very limited after 17 days (only 11% of total U). All of the above observations indicate that the addition of phosphate inhibits bioreduction of HUP.

Reduced U^{IV} Speciation. The EXAFS data from the most reduced sample (BGB) were analyzed to determine the atomic coordination of U^{IV}. Figure 4 compares the Fourier transform of the data to those from U^{IV} species characterized in previous studies.[7,8,68] The peak at R + Δ = 3.7 Å (Figure 4d) has been shown to result from the U−U coordination in uraninite.[7,8] This peak is absent in Figure 4a, indicating that the U^{IV} endmember species are not uraninite. Spectrum 4a is also different from that of carbonate-complexed U^{IV} determined in a previous study[7] (Figure 4c). The significant similarity of the spectrum in Figure 4a to that from the previously characterized U^{IV}-phosphate complex (Figure 4b) suggests the predominance of phosphate-complexed U^{IV} in our system. Shell-by-shell analysis (Supporting Information) indicates that the peak at R + Δ = 2.7 Å is due to U^{IV}−P coordination at a distance of 3.1 Å resulting from bidentate U^{IV}-phosphate complexation. The structure of this U^{IV} phosphate complex is similar to that in the

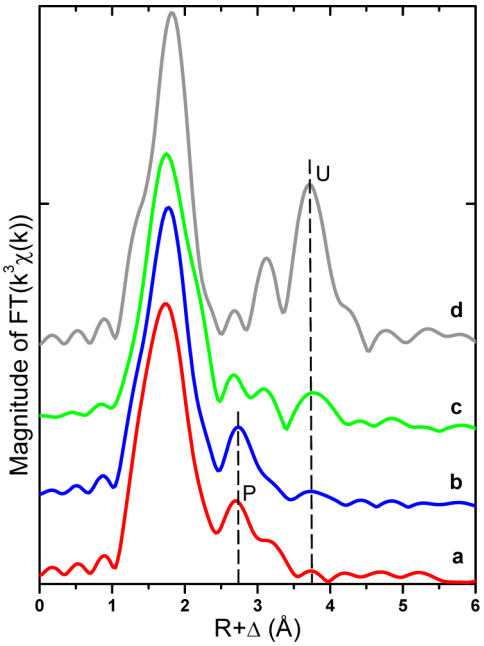

Figure 4. Fourier transform of U L_{III}-edge EXAFS data from the most reduced U^{IV} species (BGB, see Table 1) compared to standards: (a) sample BGB (this study); (b) U^{IV} produced from reduction of aqueous U^{VI} carbonate by *Desulfitobacterium* spp. in the presence of phosphate;[7,68] (c) U^{IV} produced from aqueous U^{VI} carbonate by *Desulfitobacterium* spp. in the absence of phosphate;[7] (d) nanoparticulate uraninite standard. Fourier transforms are over the range k = 2.2−10.4 $Å^{-1}$ for Hanning window sills 1.0 $Å^{-1}$ wide. Features noted by vertical lines are discussed in the text; the peak at R + Δ ∼ 3.7 Å is due to a U coordination shell, while the peak at R + Δ ∼ 2.7 Å is due to a P shell.

mineral ningyoite [$CaU(PO_4)_2 \cdot H_2O$].[69] However, our systems lacked sufficient Ca for stoichiometric ningyoite formation (Ca:U < 7%), and synchrotron X-ray diffraction did not indicate its presence in the reacted solids (data not shown). This suggests that the observed U^{IV}-phosphate or -phosphoryl species may be isolated molecular complexes adsorbed to the

solids or that an amorphous U^{IV} phosphate solid similar to ningyoite was formed, with cations other than Ca^{2+} providing charge balance in the structure. The bacteria studied here have been shown to reduce aqueous U^{VI} species to uraninite in a phosphate-free, bicarbonate-buffered medium.[7,8,10,11] The lack of uraninite as a significant endmember species in our system and the lack of dependence of the U^{IV} product on the metal-reducing bacterial species or the presence of carbonate suggest strong control by phosphate on U^{IV} speciation, with P:U ratios as low as 1:1 inhibiting uraninite formation and leading to phosphate-complexed U^{IV}.

Aqueous Uranium. The ICP analyses of the supernatants from the biogenic HUP reactors without added phosphate showed 3−9 μM U in the aqueous phase (Table 1). To evaluate whether these concentrations represented aqueous U^{VI} in equilibrium with HUP, the HUP materials were suspended in solutions identical to those in the bioreduction experiments but without inoculation with the metal-reducing bacteria (termed dissolution controls). In HEPES buffer, the measured aqueous U concentration after 20 days was 6.13 ± 0.05 μM in the biogenic HUP control compared to 4.96 ± 0.03 μM in the abiotic HUP control. In bicarbonate buffer, the concentration of U in solution increased dramatically to 37.56 ± 0.04 μM for the biogenic mineral. An increase was also observed with the abiotic mineral, with 13.61 ± 0.05 μM U detected in the solution. These results indicate that the presence of bicarbonate in the system supports higher aqueous U concentrations: about 6 times higher for the biogenic HUP and about 2.7 times higher for the abiotic HUP in our study. The trend is consistent with thermodynamic calculations showing increased solubility of uranyl phosphate minerals above pH 4 in the presence of bicarbonate (Figures S15−17 in ref 7). Under the conditions of our experiments, the biogenic HUP mineral was more soluble than abiotic HUP, supporting about 1.3 times higher aqueous U^{VI} concentrations in HEPES buffer and about 3 times higher U^{VI} concentrations in bicarbonate buffer. Higher solubility of biogenic HUP relative to abiotic HUP was also reported by Dunham-Cheatham et al.[55] and attributed to the smaller size of the biogenic HUP particles. Higher U concentrations measured in our dissolution controls correlate with larger reduction extents in the bioreduction reactors, the only exception to this trend being samples BSH vs ASB (Figure 3). This correlation may be interpreted as HUP solubility controlling the extent of U^{VI} bioreduction; however, the lower U concentrations measured in the bioreduction reactors relative to the corresponding dissolution controls indicate that aqueous U is undersaturated with respect to HUP precipitation during the bioreduction process (i.e., the system is not at equilibrium). The latter suggests that the relative rates of HUP dissolution vs the rates of dissolved U^{VI} bioreduction and removal from solution need to be considered in interpreting the observed overall extents of reduction, as discussed below.

Mechanism of U^{VI} Reduction. The majority of related microbial U^{VI} reduction studies[7−13,59,61−63] have provided U^{VI} as dissolved species. Of the remainder, only a few have explicitly examined the bioreduction of well-defined, sparingly soluble U^{VI} mineral phases.[53,60,70−72] Microbial respiration with solid-phase electron acceptors requires different mechanisms for electron transfer compared to respiration with soluble terminal electron acceptors that are easily transported into the cell (e.g., molecular oxygen, nitrate, sulfate, etc.). In the case of sparingly soluble Fe^{III} oxides, some dissimilatory Fe^{III}-reducing bacteria (DIRB) transfer electrons to Fe^{III} oxides by direct physical contact with the oxide surface, whether by means of reductases located on the outer membrane of Gram-negative bacteria such as *Geobacter* and *Shewanella*[73] or by electrically conductive appendages (often described as nanowires).[74,75] However, the need for physical contact with the Fe^{III} oxide can be readily overcome. The dissolution of Fe^{III} oxides is promoted by exogenous and endogenous ligands, and the resulting soluble Fe^{III} complexes can diffuse away from the oxide and be reduced by DIRB at a distance.[76,77] Likewise, the transfer of electrons from the cell to external electron acceptors like Fe^{III} oxides can be facilitated by soluble electron shuttles[78] that can be reversibly oxidized and reduced; the oxidized form of the electron shuttle is reduced by the organism and, in its reduced form, can transfer electrons to the Fe^{III} oxide at a distance and become reoxidized. Although they are not wholly conclusive, our results do provide the basis for informed speculation on the bioreduction of U^{VI} in our experimental systems with respect to the mechanism of electron transfer — whether the U^{VI} in HUP is reduced predominantly via electron transfer directly to the solid phase U^{VI} (designated as "solid-U^{VI}") or is reduced as a dissolved or adsorbed species after HUP dissolution (designated as "dissolved-U^{VI}").

A consistently greater extent of reduction was observed with biogenic HUP than with abiotic HUP for all three metal reducers examined in this study. This may be the result of differences in particle size between biotic and abiotic HUP. In previous work, the biogenic HUP particles were found to have a platy morphology, with lengths of 10−30 nm and thickness of 1−5 nm, while the abiotically formed HUP particles had a similar morphology but larger particle size, with lengths of 50−150 nm and thickness of about 10 nm.[55] For freely suspended particles in solution, smaller particles would be expected to increase the extent of U^{VI} reduction for a solid-U^{VI} reduction mechanism because of larger exposed surface area. However, biogenic HUP was added as particles agglomerated at the cell wall surface of *B. subtilis*, creating a thin coat of HUP (see Dunham-Cheatham et al.,[55] Figure 3). Such agglomeration effectively limits the area of biogenic HUP available for direct contact with metal-reducing bacteria to the surface area of *B. subtilis* cells. In contrast, abiotic HUP was added as freely suspended particles so their entire surface area is available for direct contact with the metal reducing bacteria or with the solution. Estimates made by using the average size and morphology of *B. subtilis* cells and the HUP particles indicate that the surface area of the biogenic HUP is 4 times that of abiotic HUP for freely suspended particles. However, the *effective* area for direct contact with *B. subtilis*-associated HUP is up to 27 times *smaller*. (Details of the calculations are provided in the Supporting Information.) Since the rate of U^{VI} reduction by the solid-U^{VI} reduction mechanism is expected to be proportional to the surface area available for direct contact, one would expect a smaller extent of reduction with the biogenic HUP relative to the abiotic HUP (at any given time), which is contrary to our results. Conversely, for a dissolved-U^{VI} reduction mechanism, the extent of U^{VI} reduction at any given time will be correlated with the HUP dissolution rate and the dissolved U^{VI} reduction rate. Because HUP particles associated with the *B. subtilis* cells are not encapsulated, a large proportion of their surface area remains in contact with the solution. The greater surface area of biogenic HUP in contact with solution would result in a greater extent of U^{VI} reduction for a dissolved-U^{VI} reduction mechanism controlled by the mineral dissolution rate. It is also possible that biogenic

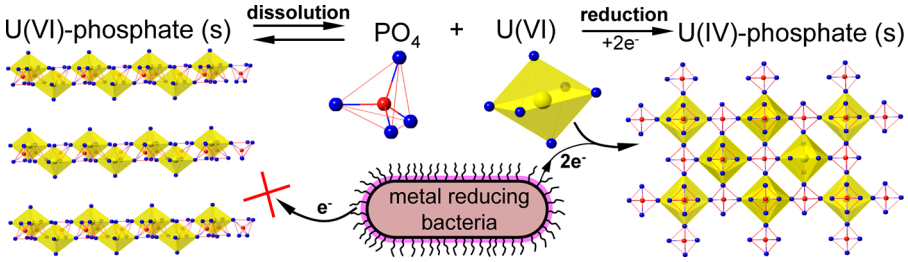

Figure 5. Schematic of the proposed HUP bioreduction mechanism. Uranium atoms are in yellow, O atoms are in blue, P atoms are in red. Electrons are transferred from the bacteria to the dissolved or bacterially adsorbed species of U formed after HUP dissolution, instead of directly to the mineral surface. Reduction is followed by precipitation of U^{IV} phosphate. The data for the crystal structures of U^{VI} phosphate and U^{IV} phosphate were obtained from Morosin et al.[89] and Dusausoy et al.[69]

HUP had a higher intrinsic dissolution rate than abiotitc HUP. Alternatively, for a dissolved-U^{VI} reduction mechanism controlled by the equilibrium U^{VI} concentration, the higher dissolved U^{VI} concentrations observed in the biogenic relative to abiotic HUP systems would be expected to result in a greater extent of U^{VI} reduction for biogenic HUP. Indeed, we observed a greater extent of reduction of biogenic HUP consistent with a dissolved-U^{VI} reduction mechanism, as illustrated in Figure 5.

Support for the dissolved-U^{VI} reduction mechanism is also provided by the effect of carbonate and phosphate concentrations on the extent of U^{VI} reduction. Results for the dissolution controls show that the presence of carbonate supports higher aqueous U^{VI} concentrations, whereas the presence of additional phosphate inhibits HUP dissolution. These trends correlate well with the observed extents of U^{VI} reduction, supporting a dissolved-U^{VI} reduction mechanism controlled by the steady-state U^{VI} concentration. Alternatively, if one assumes a dissolved-U^{VI} reduction mechanism controlled by the mineral dissolution rate, then the presence of carbonate is also expected to result in a larger extent of U^{VI} reduction, because carbonate has been shown to increase the concentration of U in solution and the rate of U^{VI} mineral dissolution.[47,79−81] We did not measure dissolution rates for phosphate minerals in the presence of phosphate and did not find them in the literature. However, slower HUP dissolution would be expected in phosphate-amended solutions because of the higher activity of dissolved phosphate species. For assumed mineral dissolution control of U^{VI} bioreduction, the lower HUP reduction extent observed here with added phosphate again supports a dissolved-U^{VI} reduction mechanism.

Additional insight into the relative importance of HUP dissolution vs dissolved-U^{VI} reduction in determining the overall rate of HUP bioreduction can be inferred from the measured U concentrations and the aqueous U^{VI} reduction rates observed in previous studies. The aqueous U^{VI} concentrations in equilibrium with biogenic or abiotic HUP measured in the bicarbonate-buffered dissolution controls were 38 and 14 μM, respectively, whereas aqueous U concentrations measured during the ongoing HUP bioreduction were only 3−9 μM (Table 1 and "dissolved uranium" discussion above). Aqueous U concentrations that are lower than the U concentrations in equilibrium with the mineral suggest that HUP dissolution is slower than the reduction of dissolved U^{VI} and that dissolution is the rate-limiting step. Once U^{VI} is dissolved in solution, the presence or absence of phosphate does not appreciably alter the U^{VI} species distribution in 30 mM bicarbonate because of the prevalence of U^{VI}-carbonate complexes at pH ∼7 (see speciation calculations in the Supporting Information), which suggests that the aqueous U^{VI} reduction rates in our system should be similar to those in previous studies. Only 24−72 h were necessary for complete removal of 50−1400 μM aqueous U^{VI} by *Shewanella, Anaeromyxobacter,* or *Geobacter* spp. in 30 mM bicarbonate medium without Ca^{2+}.[10,23,63,82−84] The limited reduction of HUP observed here over 10−20 days is in contrast to the fast aqueous U^{VI} bioreduction established previously, again suggesting that mineral dissolution is the rate-limiting step. Note that the aqueous reduction step still affects the overall rate, even if it is not rate-limiting. This is evident from the different reduction extents observed in the incubations with the three bacterial species (Figure 3). The latter can be rationalized in terms of different reduction rates for dissolved U^{VI} affecting the HUP dissolution kinetics by controlling the amount of product in the dissolution reaction (i.e., the degree of saturation in the solution). Indeed, a correlation can be observed between the measured U^{VI} concentrations in solution and the overall reduction extent observed in reactors with bicarbonate — the extent of reduction was more limited with *Anaeromyxobacter* where higher transient U concentrations were also observed (Table 1, Figure 3). In other words, faster bioreduction of the dissolved U^{VI} species leads to lower aqueous U^{VI} concentrations, which in turn promote faster HUP dissolution, resulting in higher overall reduction rates.

The preferential reduction of dissolved U^{VI} species over solid-phase U^{VI} in our experimental systems would not be expected *a priori*. As mentioned previously, *Geobacter* and *Shewanella* spp. are known to transfer electrons to Fe^{III} oxides by direct physical contact with the oxide surface, whether by means of reductases located on the outer membrane[73] or by electrically conductive appendages.[74,75] Even though *Anaeromyxobacter*, *Geobacter*, and *Shewanella* can respire by using solid-phase Fe^{III} oxides as electron acceptors, our results are consistent with reduction of U^{VI} in HUP primarily via the dissolved-U^{VI} reduction mechanism, consistent with the dissolution/reduction pathway reported for reduction of U^{VI} in sodium boltwoodite ($NaUO_2SiO_3OH \bullet 1.5\ H_2O$) by *S. oneidensis* MR-1.[70,85] The results suggest different enzymatic mechanisms for solid phase U^{VI}- vs Fe^{III}-reduction by these bacteria.

Environmental Significance. Understanding the mechanisms, kinetics, and controls on U^{VI} bioreduction under the various conditions possible in natural and engineered systems (e.g., phosphate amendments) contributes to our ability to predict and control the migration of U in contaminated environments and provides insight into electron transfer from metal-reducing bacteria to soluble or solid-phase electron acceptors. The slow bioreduction of phosphate-precipitated U^{VI} observed here and also in Khijniak et al.[53] establishes reduction

as a potential pathway for further U transformations after field-site phosphate amendments. It also indicates that excess phosphate may slow down U^{VI} reduction during bioremediation. The observed enhancement effect of bicarbonate on the reduction extent suggests a way to speed up bioreduction of solid-phase U^{VI}. The latter, however, should be balanced with the decrease in bioreduction rates of aqueous U^{VI} in the presence of Ca and bicarbonate.[82] The effectiveness of phosphate amendments for long-term immobilization of U at contaminated sites is predicated on the stability of the resultant U^{VI} phosphate phases. The formation of bioreduced U^{IV} species that are similar to ningyoite (and different from uraninite) raises new questions about the stability of U^{IV} phases.[7,50,57,61,68,86] Ningyoite was originally identified as the main ore component in an unoxidized zone of the Ningyo-toge mine, Tottori Prefecture, Japan, and was thought to be unique to this region;[87] it has since been identified in ore deposits in North America, Europe, and Asia[88] and is the most commonly occurring and best characterized of the U^{IV} phosphate minerals. Despite this, there is a paucity of data relevant to understanding and predicting the geochemical behavior of ningyoite and related U^{IV}-phosphate phases. Ningyoite appears to be less soluble than HUP.[58] Therefore, the bioreduction of uranyl phosphates to ningyoite or ningyoite-like phases could further limit U mobility. However, as with uraninite, ningyoite is susceptible to oxidation if anoxic conditions are not maintained. More information on the geochemical behavior of ningyoite and related uranous phosphate phases under environmentally relevant conditions is needed to properly assess their impact on the fate of U in reducing subsurface environments, during or after remediation approaches based on phosphate amendment.

■ ASSOCIATED CONTENT

Ⓢ Supporting Information

HUP synthesis and characterization, bacterial culturing and reactor setup, XANES/EXAFS measurement and analysis procedures, surface area estimation calculations, and aqueous U^{VI} speciation calculations are described in more detail. This material is available free of charge via the Internet at http://pubs.acs.org.

■ AUTHOR INFORMATION

Corresponding Author

*Phone: 630-252-8242. Fax: 630-252-9793. E-mail: mboyanov@anl.gov. Corresponding author address: Biosciences Division, Argonne National Laboratory, 9700 South Cass Avenue, Bldg. 203, Argonne, IL 60439-4843.

Author Contributions

⊥These authors contributed equally to this work.

Notes

The authors declare no competing financial interest.

■ ACKNOWLEDGMENTS

We thank B. Mishra and the MRCAT/EnviroCAT beamline staff for assistance during EXAFS data collection. M. J. Kwon was supported by an Argonne Director's Fellowship and the KIST-Gangneung Institute (Grant 2Z03860). This research is part of the Subsurface Science Scientific Focus Area at Argonne National Laboratory supported by the DOE Subsurface Biogeochemical Research Program, Office of Biological and Environmental Research, Office of Science, under contract DE-AC02-06CH11357. Use of the Advanced Photon Source, a user facility operated for the DOE Office of Science by Argonne National Laboratory, was supported by DOE under contract DE-AC02-06CH11357. MRCAT/EnviroCAT operations are supported by DOE and the MRCAT/EnviroCAT member institutions.

■ REFERENCES

(1) Markich, S. J. Uranium speciation and bioavailability in aquatic systems: an overview. *TheScientificWorldJournal* **2002**, *2*, 707−729.

(2) O'Loughlin, E. J.; Boyanov, M. I.; Antonopoulos, D. A.; Kemner, K. M. Redox processes affecting the speciation of technetium, uranium, neptunium, and plutonium in aquatic and terrestrial environments. In *Aquatic Redox Processes*; Tratnyek, P. G., Grundl, T. J., Haderlein, S. B., Eds.; American Chemical Society: Washngton, DC, 2011; Vol. *1071*, pp 477−517.

(3) Wall, J. D.; Krumholz, L. R. Uranium reduction. *Annu. Rev. Microbiol.* **2006**, *60*, 149−166.

(4) Wazne, M.; Korfiatis, G. P.; Meng, X. Carbonate effects on hexavalent uranium adsorption by iron oxyhydroxide. *Environ. Sci. Technol.* **2003**, *37* (16), 3619−3624.

(5) Zhou, P.; Gu, B. Extraction of oxidized and reduced forms of uranium from contaminated soils: Effects of carbonate concentrations and pH. *Environ. Sci. Technol.* **2005**, *39* (12), 4435−4440.

(6) Abdelouas, A.; Lu, Y.; Lutze, W.; Nuttall, H. E. Reduction of U(VI) to U(IV) by indigenous bacteria in contaminated ground water. *J. Contam. Hydrol.* **1998**, *35* (1−3), 217−233.

(7) Boyanov, M. I.; Fletcher, K. E.; Kwon, M. J.; Rui, X.; O'Loughlin, E. J.; Löffler, F. E.; Kemner, K. M. Solution and microbial controls on the formation of reduced U(IV) phases. *Environ. Sci. Technol.* **2011**, *45* (19), 8336−8344.

(8) Burgos, W. D.; McDonough, J. T.; Senko, J. M.; Zhang, G.; Dohnalkova, A. C.; Kelly, S. D.; Gorby, Y.; Kemner, K. M. Characterization of uraninite nanoparticles produced by *Shewanella oneidensis* MR-1. *Geochim. Cosmochim. Acta* **2008**, *72* (20), 4901−4915.

(9) Lovley, D. R.; Phillips, E. J. P.; Gorby, Y. A.; Landa, E. R. Microbial reduction of uranium. *Nature* **1991**, *350* (6317), 413−416.

(10) Marshall, M. J.; Dohnalkova, A. C.; Kennedy, D. W.; Plymale, A. E.; Thomas, S. H.; Löffler, F. E.; Sanford, R. A.; Zachara, J. M.; Fredrickson, J. K.; Beliaev, A. S. Electron donor-dependent radionuclide reduction and nanoparticle formation by *Anaeromyxobacter dehalogenans* strain 2CP-C. *Environ. Microbiol.* **2009**, *11* (2), 534−543.

(11) Sharp, J. O.; Schofield, E. J.; Veeramani, H.; Suvorova, E. I.; Kennedy, D. W.; Marshall, M. J.; Metha, A.; Bargar, J. R.; Bernier-Latmani, R. Structural similarities between biogenic uraninites produced by phylogenetically and metabolically diverse bacteria. *Environ. Sci. Technol.* **2009**, *43* (21), 8295−8301.

(12) Singer, D. A.; Farges, F.; Brown, G. E., Jr. Biogenic nanoparticulate UO_2: Synthesis, characterization, and factors affecting surface reactivity. *Geochim. Cosmochim. Acta* **2009**, *73*, 3593−3611.

(13) Veeramani, H.; Schofield, E. J.; Sharp, J. O.; Suvorova, E. I.; Ulrich, K.-U.; Metha, A.; Giammar, D. E.; Bargar, J. R.; Bernier-Latmani, R. Effect of Mn(II) on the structure and reactivity of biogenic uraninite. *Environ. Sci. Technol.* **2009**, *43* (17), 6541−6547.

(14) Wu, W.-M.; Carley, J.; Luo, J.; Ginder-Vogel, M. A.; Cardenas, E.; Leigh, M. B.; Hwang, C.; Kelly, S. D.; Ruan, C.; Wu, L.; van Nostrand, J.; Gentry, T.; Lowe, K.; Melhorn, T.; Carroll, S.; Luo, W.; Fields, M. W.; Gu, B.; Watson, D.; Kemner, K. M.; Marsh, T.; Tiedje, J.; Zhou, J.; Fendorf, S.; Kitanidis, P. K.; Jardine, P. M.; Criddle, C. S. In situ bioreduction of uranium(VI) to submicromolar levels and reoxidation by dissolved oxygen. *Environ. Sci. Technol.* **2007**, *41* (16), 5716−5723.

(15) Yabusaki, S. B.; Fang, Y.; Long, P. E.; Resch, C. T.; Peacock, A. D.; Komlos, J.; Jaffe, P. R.; Morrison, S. J.; Dayvault, R. D.; White, D. C.; Anderson, R. T. Uranium removal from groundwater via in situ biostimulation: Field-scale modeling of transport and biological processes. *J. Contam. Hydrol.* **2007**, *93* (1−4), 216−235.

(16) Beller, H. R. Anaerobic, nitrate-dependent oxidation of U(VI) oxide minerals by the chemolithoautotrophic bacterium *Thiobacillus denitrificans*. *Appl. Environ. Microbiol.* **2005**, *71* (4), 2170−2174.
(17) Finneran, K. T.; Housewright, M. E.; Lovley, D. R. Multiple influences of nitrate on uranium solubility during bioremediation of uranium-contaminated subsurface sediments. *Environ. Microbiol.* **2002**, *4* (9), 510−516.
(18) Fredrickson, J. K.; Zachara, J. M.; Kennedy, D. W.; Liu, C.; Duff, M. C.; Hunter, D. B.; Dohnalkova, A. Influence of Mn oxides on the reduction of uranium(VI) by the metal-reducing bacterium *Shewanella putrefaciens*. *Geochim. Cosmochim. Acta* **2002**, *66* (18), 3247−3262.
(19) Ginder-Vogel, M.; Stewart, B.; Fendorf, S. Kinetic and mechansitic constraints on the oxidation of biogenic uraninite by ferrihydrite. *Environ. Sci. Technol.* **2010**, *44* (1), 163−169.
(20) Komlos, J.; Peacock, A.; Kukkadapu, R. K.; Jaffé, P. R. Long-term dymanics of uranium reduction/reoxidation under low sulfate conditions. *Geochim. Cosmochim. Acta* **2008**, *72* (15), 3603−3615.
(21) Sani, R. K.; Peyton, B. M.; Dohnalkova, A.; Amonette, J. E. Reoxidation of reduced uranium with iron(III) (hydr)oxides under sulfate-reducing conditions. *Environ. Sci. Technol.* **2005**, *39* (7), 2059−2066.
(22) Senko, J. M.; Istok, J. D.; Suflita, J. M.; Krumholz, L. R. In-situ evidence for uranium immobilization and remobilization. *Environ. Sci. Technol.* **2002**, *36* (7), 1491−1496.
(23) Senko, J. M.; Kelly, S. D.; Dohnalkova, A. C.; McDonough, J. T.; Kemner, K. M.; Burgos, W. D. The effect of U(VI) bioreduction kinetics on subsequent reoxidation of biogenic U(IV). *Geochim. Cosmochim. Acta* **2007**, *71* (19), 4644−4654.
(24) Senko, J. M.; Mohamed, Y.; Dewers, T. A.; Krumholz, L. R. Role for Fe(III) minerals in nitrate-dependent microbial U(VI) oxidation. *Environ. Sci. Technol.* **2005**, *39* (8), 2529−2536.
(25) Weber, K. A.; Thrash, J. C.; Van Trump, J. I.; Achenbach, L. A.; Coates, J. D. Environmental and taxanomic bacterial diversity of anaerobic uranium(IV) bio-oxidation. *Appl. Environ. Microbiol.* **2011**, *77* (13), 4693−4696.
(26) Arey, J. S.; Seaman, J. C.; Bertsch, P. M. Immobilization of uranium in contaminated sediments by hydroxyapatite addition. *Environ. Sci. Technol.* **1999**, *33* (2), 337−342.
(27) Beazley, M. J.; Martinez, R. J.; Sobecky, P. A.; Webb, S. M.; Taillefert, M. Uranium biomineralization as a result of bacterial phosphatase activity: Insights from bacterial isolates from a contaminated subsurface. *Environ. Sci. Technol.* **2007**, *41* (16), 5701−5707.
(28) Beazley, M. J.; Martinez, R. J.; Sobecky, P. A.; Webb, S. M.; Taillefert, M. Nonreductive biomineralization of uranium(VI) phosphate via microbial phosphatase activity in anaerobic conditions. *Geomicrobiol. J.* **2009**, *26*, 431−441.
(29) Beazley, M. J.; Martinez, R. J.; Webb, S. M.; Sobecky, P. A.; Taillefert, M. The effect of pH and natural microbial phosphatase activity on the speciation of uranium in subsurface soils. *Geochim. Cosmochim. Acta* **2011**, *75*, 5648−5663.
(30) Fuller, C. C.; Bargar, J. R.; Davis, J. A.; Piana, M. J. Mechanisms of uranium interactions with hydroxyapatite: Implications for groundwater remediation. *Environ. Sci. Technol.* **2002**, *36* (2), 158−165.
(31) Macaskie, L. E.; Empson, R. M.; Cheetham, A. K.; Grey, C. P.; Skarnulis, A. J. Uranium bioaccumulation by a *Citrobacter* sp. as a result of enzymatically mediated growth of polycrystalline HUO_2PO_4. *Science* **1992**, *257*, 782−784.
(32) Martinez, R. J.; Beazley, M. J.; Taillefert, M.; Arakaki, A. K.; Skolnick, J.; Sobecky, P. A. Aerobic uranium (VI) bioprecipitation by metal-resistant bacteria isolated from radionuclide- and metal-contaminated subsurface soils. *Environ. Microb.* **2007**, *9* (12), 3122−3133.
(33) Naftz, D. L.; Morrison, S. J.; Feltcorn, E. M.; Freethey, G. W.; Fuller, C. C.; Piana, M. J.; Wilhelm, R. G.; Rowland, R. C.; Davis, J. A.; Blue, J. E. Field demonstration of permeable reactive barriers to remove dissolved uranium from groundwater, Fry Canyon, Utah, U.S. EPA, 2000.
(34) Ohnuki, T.; Kozai, N.; Samadfam, M.; Yasuda, R.; Yamamoto, S.; Narumi, K.; Naramoto, H.; Murakami, T. The formation of autunite ($Ca(UO_2)_2(PO_4)_2{*}nH_2O$) within the leached layer of dissolving apatite: incorporation mechanism of uranium by apatite. *Chem. Geol.* **2004**, *211* (1−2), 1−14.
(35) Shelobolina, E. S.; Konishi, H.; Xu, H.; Roden, E. E. U(VI) sequestration in hydroxyapatite produced by microbial glycerol 3-phosphate metabolism. *Appl. Environ. Microbiol.* **2009**, *75* (18), 5773−5778.
(36) Singh, A.; Ulrich, K.-U.; Giammar, D. E. Impact of phosphate on U(VI) immobilization in the presence of goethite. *Geochim. Cosmochim. Acta* **2010**, *74* (22), 6324−6343.
(37) Wellman, D. M.; Pierce, E. M.; Richards, E. L.; Butler, B. C.; Parker, K. E.; Glovack, J. N.; Burton, S. D.; Baum, S. R.; Clayton, E. T.; Rodriguez, E. A. Interim report: Uranium stabilization through polyphosphate injection; Pacific Northwest National Laboratory, 2007.
(38) Wellman, D. M.; Pierce, E. M.; Valenta, M. M. Efficacy of soluble sodium tripolyphosphate amendments for the in-situ immobilization of uranium. *Environ. Chem.* **2007**, *4* (5), 293−300.
(39) Zheng, Z.; Wan, J.; Song, X.; Tokunaga, T. K. Sodium meta-autunite colloids: Synthesis, characterization, and stability. *Colloids Surf., A* **2006**, *274* (1−3), 48−55.
(40) Finch, R.; Murakami, T. Systematics and paragenesis of uranium minerals. In *Uranium: Mineralogy, geochemistry and the environment*; Burns, P. C., Finch, R., Eds.; Mineralogical Society of America: Washington, DC., 1999; Vol. *38*, pp 91−179.
(41) Catalano, J. G.; McKinley, J. P.; Zachara, J. M.; Heald, S. M.; Smith, S. C.; Brown, G. E., Jr. Changes in uranium speciation through a depth sequence of contaminated Hanford sediments. *Environ. Sci. Technol.* **2006**, *40* (8), 2517−2524.
(42) Francis, A. J.; Dodge, C. J. Remediation of soils and wastes contaminated with uranium and toxic metals. *Environ. Sci. Technol.* **1998**, *32* (24), 3993−3998.
(43) Jerden, J. L.; Sinha, A. K. Phosphate based immobilization of uranium in an oxidizing bedrock aquifer. *Appl. Geochem.* **2003**, *18* (6), 823−843.
(44) Sato, T.; Murakami, T.; Yanase, N.; Isobe, H.; Payne, T. E.; Airey, P. L. Iron nodules scavenging uranium from groundwater. *Environ. Sci. Technol.* **1997**, *31* (10), 2854−2858.
(45) Hamdali, H.; Bouizgarne, B.; Hafidi, M.; Lebrihi, A.; Virolle, M. J.; Ouhdouch, Y. Screening for rock phosphate solubilizing *Actinomycetes* from Moroccan phosphate mines. *Appl. Soil Ecol.* **2008**, *38* (1), 12−19.
(46) Hutchens, E.; Valsami-Jones, E.; Harouiya, N.; Chaïrat, C.; Oelkers, E. H.; McEldoney, S. An experimental investigation of the effect of *Bacillus megateriumon* on apatite dissolution. *Geochem. J.* **2006**, *23* (3−4), 177−182.
(47) Katsenovich, Y. P.; Carvajal, D. A.; Wellman, D. M.; Lagos, L. E. Enhanced U(VI) release from autunite mineral by aerobic *Arthrobacter* sp. in the presence of aqueous bicarbonate. *Chem. Geol.* **2012**, *308*−*309*, 1−9.
(48) Welch, S. A.; Taunton, A. E.; Banfield, J. F. Effect of microorganisms and microbial metabolites on apatite dissolution. *Geochem. J.* **2002**, *19* (3), 343−367.
(49) Ray, A. E.; Bargar, J. R.; Sivaswamy, V.; Dohnalkova, A. C.; Fujita, Y.; Peyton, B. M.; Magnuson, T. S. Evidence for multiple modes of uranium immobilization by an anaerobic bacterium. *Geochim. Cosmochim. Acta* **2011**, *75* (10), 2684−2695.
(50) Sivaswamy, V.; Boyanov, M. I.; Peyton, B. M.; Viamajala, S.; Gerlach, R.; Apel, W. A.; Sani, R. K.; Dohnalkova, A.; Kemner, K. M.; Borch, T. Multiple mechanisms of uranium immobilization by *Cellulomonas* sp. strain ES6. *Biotechnol. Bioeng.* **2011**, *108* (2), 264−276.
(51) Smeaton, C. M.; Weisener, C. G.; Burns, P. C.; Fryer, B. J.; Fowle, D. A. Bacterially enhanced dissolution of meta-autunite. *Am. Mineral.* **2008**, *93*, 1858−1864.
(52) Wade, R., Jr.; DiChristina, T. J. Isolation of U(VI) reduction-deficient mutants of *Shewanella putrefaciens*. *FEMS Microbiol. Lett.* **2000**, *184* (2), 143−148.

(53) Khijniak, T. V.; Slobodkin, A. I.; Coker, V.; Renshaw, J. C.; Livens, F. R.; Bonch-Osmolovskaya, E. A.; Birkeland, N.-K.; Medvedeva-Lyalikova, N. N.; Lloyd, J. R. Reduction of uranium(VI) phosphate during growth of the thermophilic bacterium *Thermoterrabacterium ferrireducens*. *Appl. Environ. Microbiol.* **2005**, *71* (10), 6423−6426.

(54) Benzerara, K.; Miot, J.; Morin, G.; Ona-Nguema, G.; Skouri-Panet, F.; Ferard, C. Significance, mechanisms and environmental implications of microbial biomineralization. *C. R. Geosci.* **2011**, *343* (2−3), 160−167.

(55) Dunham-Cheatham, S.; Rui, X.; Bunker, B. A.; Menguy, N.; Hellmann, R.; Fein, J. The effects of non-metabolizing bacterial cells on the precipitation of U, Pb and Ca phosphates. *Geochim. Cosmochim. Acta* **2011**, *75*, 2828−2847.

(56) Macaskie, L. E.; Bonthrone, K. M.; Yong, P.; Goddard, D. T. Enzymically mediated bioprecipitation of uranium by a *Citrobacter* sp.: a concerted role for exocellular lipopolysaccharide and associated phosphatase in biomineral formation. *Microbiology (Reading, U. K.)* **2000**, *146*, 1855−1867.

(57) Bernier-Latmani, R.; Veeramani, H.; Vecchia, E. D.; Junier, P.; Lezama-Pacheco, J. S.; Suvorova, E. I.; Sharp, J. O.; Wigginton, N. S.; Bargar, J. R. Non-uraninite products of microbial U(VI) reduction. *Environ. Sci. Technol.* **2010**, *44* (24), 9456−9462.

(58) Muto, T. Thermochemical stability of ningyoite. *Mineral. J.* **1965**, *4* (4), 245−274.

(59) Caccavo, F., Jr.; Lonergan, D. J.; Lovley, D. R.; Davis, M.; Stolz, J. F.; McInerney, M. J. *Geobacter sulfurreducens* sp. nov., a hydrogen- and acetate-oxidizing dissimilatory metal-reducing microorganism. *Appl. Environ. Microbiol.* **1994**, *60* (10), 3752−3759.

(60) Fredrickson, J. K.; Zachara, J. M.; Kennedy, D. W.; Duff, M. C.; Gorby, Y. A.; Li, S.-M. W.; Krupka, K. M. Reduction of U(VI) in goethite (α-FeOOH) suspensions by a dissimilatory metal-reducing bacterium. *Geochim. Cosmochim. Acta* **2000**, *64* (18), 3085−3098.

(61) Lee, S. Y.; Baik, M. H.; Choi, J. W. Biogenic formation and growth of uraninite (UO_2). *Environ. Sci. Technol.* **2010**, *44* (22), 8409−8414.

(62) Sanford, R. A.; Wu, Q.; Sung, Y.; Thomas, S. H.; Amos, B. K.; Prince, E. K.; Löffler, F. E. Hexavalent uranium supports growth of *Anaeromyxobacter dehalogenans* and *Geobacter* spp. with lower than predicted biomass yields. *Environ. Microbiol.* **2007**, *9* (11), 2885−2893.

(63) Shelobolina, E. S.; Coppi, M. V.; Korenevsky, A. A.; DiDonato, L. N.; Sullivan, S. A.; Konishi, H.; Xu, H.; Leang, C.; Butler, J. E.; Kim, B. H.; Lovley, D. R. Importance of *c*-type cytochromes for U(VI) reduction by *Geobacter sulfurreducens*. *BMC Microbiol.* **2007**, *7* (16), 1−15.

(64) Kropf, A. J.; Katsoudas, J.; Chattopadhyay, S.; Shibata, T.; Lang, E. A.; Zyryanov, V. N.; Ravel, B.; McIvor, K.; Kemner, K. M.; Scheckel, K. G.; Bare, S. R.; Terry, J.; Kelly, S. D.; Bunker, B. A.; Segre, C. U.; Garrett, R.; Gentle, I.; Nugent, K.; Wilkins, S. The new MRCAT (Sector 10) bending magnet beamline at the Advanced Photon Source. *AIP Conf. Proc.* **2010**, *1234*, 299−302.

(65) Boyanov, M. I.; O'Loughlin, E. J.; Roden, E. E.; Fein, J. B.; Kemner, K. M. Adsorption of Fe(II) and U(VI) to carboxyl-functionalized microspheres: The influence of speciation on uranyl reduction studied by titration and XAFS. *Geochim. Cosmochim. Acta* **2007**, *71* (8), 1898−1912.

(66) Hudson, E.; Rehr, J.; Bucher, J. Multiple-scattering calculations of the uranium L3-edge x-ray-absorption near-edge structure. *Phys. Rev. B* **1995**, *52* (19), 13815−13826.

(67) Kelly, S. D.; Kemner, K. M.; Fein, J. B.; Fowle, D. A.; Boyanov, M. I.; Bunker, B. A.; Yee, N. X-ray absorption fine structure determination of pH-dependent U-bacterial cell wall interactions. *Geochim. Cosmochim. Acta* **2002**, *66* (22), 3855−3871.

(68) Fletcher, K. E.; Boyanov, M. I.; Thomas, S. H.; Wu, Q.; Kemner, K. M.; Löffler, F. E. U(VI) reduction to mononuclear U(IV) by *Desulfitobacterium* species. *Environ. Sci. Technol.* **2010**, *44* (12), 4705−4709.

(69) Dusausoy, Y.; Ghermani, N. E.; Podor, R.; Cuney, M. Low-temperature ordered phase of CaU(PO4)(2): Synthesis and crystal structure. *Eur. J. Mineral.* **1996**, *8* (4), 667−673.

(70) Liu, C.; Jeon, B.-H.; Zachara, J. M.; Wang, Z.; Dohnalkova, A.; Fredrickson, J. K. Kinetics of microbial reduction of solid phase U(VI). *Environ. Sci. Technol.* **2006**, *40* (20), 6290−6296.

(71) Liu, C.; Zachara, J. M.; Zhong, L.; Heald, S. M.; Wang, Z.; Jeon, B.-H.; Fredrickson, J. K. Microbial reduction of intragrain U(VI) in contaminated sediment. *Environ. Sci. Technol.* **2009**, *43* (13), 4928−4933.

(72) Ortiz-Bernad, I.; Anderson, R. T.; Vrionis, H. A.; Lovley, D. R. Resistance of solid-phase U(VI) to microbial reduction during in situ bioremediation of uranium-contaminated groundwater. *Appl. Environ. Microbiol.* **2004**, *70* (12), 7558−7560.

(73) Shi, L.; Richardson, D. J.; Wang, Z.; Kerisit, S. N.; Rosso, K. M.; Zachara, J. M.; Fredrickson, J. K. The roles of outer membrane cytochromes of *Shewanella* and *Geobacter* in extracellular electron transfer. *Environ. Microbiol. Rep.* **2009**, *1* (4), 220−227.

(74) Gorby, Y. A.; Yanina, S.; McLean, J. S.; Rosso, K. M.; Moyles, D.; Dohnalkova, A.; Beveridge, T. J.; Chang, I. S.; Kim, B. H.; Kim, K. S.; Culley, D. E.; Reed, S. B.; Romine, M. F.; Saffarini, D. A.; Hill, E. A.; Shi, L.; Elias, D. A.; Kennedy, D. W.; Pinchuk, G.; Watanabe, K.; Ishii, S. i.; Logan, B.; Nealson, K. H.; Fredrickson, J. K. Electrically conductive bacterial nanowires produced by *Shewanella oneidensis* strain MR-1 and other microorganisms. *Proc. Natl. Acad. Sci. U. S. A.* **2006**, *103* (30), 11358−11363.

(75) Reguera, G.; McCarthy, K. D.; Metha, T.; Nicoll, J. S.; Tuominen, M. T.; Lovley, D. R. Extracellular electron transfer via microbial nanowires. *Nature* **2005**, *435* (7045), 1098−1101.

(76) Nevin, K. P.; Lovley, D. R. Mechanisms for Fe(III) oxide reduction in sedimentary environments. *Geomicrobiol. J.* **2002**, *19*, 141−159.

(77) Taillefert, M.; Beckler, J. S.; Carey, E.; Burns, J. L.; Fennessey, C. M.; DiChristina, T. J. *Shewanella putrefaciens* produces an Fe(III)-solubilizing organic ligand during anaerobic respiration on insoluble Fe(III) oxides. *J. Inorg. Biochem.* **2007**, *101*, 1760−1767.

(78) O'Loughlin, E. J. Effects of electron transfer mediators on the biodegradation of lepidocrocite (γ-FeOOH) by *Shewanella putrefaciens* CN32. *Environ. Sci. Technol.* **2008**, *42* (18), 6876−6882.

(79) Felmy, A. R.; Xia, Y.; Wang, Z. The solubility product of $NaUO_2PO_4 \cdot xH_2O$ determined in phosphate and carbonate solutions. *Radiochim. Acta* **2005**, *93* (7), 401−408.

(80) Ilton, E. S.; Liu, C.; Yantasee, W.; Wang, Z.; Moore, D. A.; Felmy, A. R.; Zachara, J. M. The dissolution of synthetic Na-boltwoodite in sodium carbonate solutions. *Geochim. Cosmochim. Acta* **2006**, *70* (19), 4836−4849.

(81) Sowder, A. G.; Clark, S. B.; Fjeld, R. A. The impact of mineralogy in the U(VI)-Ca-PO_4 system on the environmental availability of uranium. *J. Radioanal. Nucl. Chem.* **2001**, *248* (3), 517−524.

(82) Brooks, S. C.; Fredrickson, J. K.; Carroll, S. L.; Kennedy, D. W.; Zachara, J. M.; Plymale, A. E.; Kelly, S. D.; Kemner, K. M.; Fendorf, S. Inhibition of bacterial U(VI) reduction by calcium. *Environ. Sci. Technol.* **2003**, *37* (9), 1850−1858.

(83) Renshaw, J. C.; Butchins, L. J. C.; Livens, F. R.; May, I.; Charnock, J. M.; Lloyd, J. R. Bioreduction of uranium: Environmental implications of a pentavalent intermediate. *Environ. Sci. Technol.* **2005**, *39* (15), 5657−5660.

(84) Schofield, E. J.; Veeramani, H.; Sharp, J. O.; Suvorova, E.; Bernier-Latmani, R.; Metha, A.; Stahlman, J.; Webb, S. M.; Clark, D. L.; Conradson, S. D.; Ilton, E. S.; Bargar, J. R. Structure of biogenic uraninite produced by *Shewanella oneidensis* strain MR-1. *Environ. Sci. Technol.* **2008**, *42* (21), 7898−7904.

(85) Liu, C.; Jeon, B. H.; Zachara, J. M.; Wang, Z. Influence of calcium on microbial reduction of solid phase uranium(VI). *Biotechnol. Bioeng.* **2007**, *97* (6), 1415−1422.

(86) Veeramani, H.; Alessi, D. S.; Suvorova, E. I.; Lezama-Pacheco, J. S.; Stubbs, J. E.; Sharp, J. O.; Dippon, U.; Kappler, A.; Bargar, J. R.; Bernier-Latmani, R. Products of abiotic U(VI) reduction by biogenic

magnetite and vivianite. *Geochim. Cosmochim. Acta* **2011**, *75* (9), 2512−2528.
(87) Muto, T.; Meyrowitz, R.; Pommer, A. M.; Murano, T. Ningyoite, a new uranous phosphate mineral from Japan. *Am. Mineral.* **1959**, *44*, 633−650.
(88) Doinikova, O. A. Uranium deposits with a new phosphate type of blacks. *Geol. Ore Deposits (Transl. of Geol. Rudn. Mestorozhd.)* **2007**, *49* (1), 80−86.
(89) Morosin, B. Hydrogen uranyl phosphate tetrahydrate, a hydrogen-ion solid electrolyte. *Acta Crystallogr., Sect. B: Struct. Sci.* **1978**, *34* (DEC), 3732−3734.